

1 Dear Dr. Luterbacher,

2

3 My coauthors and I thank you for your invitation to revise our manuscript. Here we will
4 comment on, one-by one, the referee comments/suggestions.

5

6 Sincerely,

7 Nesibe Köse

8

9 **Response to RC1 comments**

10

11 Thank you for your time and comments, which improved our manuscript and gave us a chance to
12 discuss our results in detail.

13

14 Major comments:

15

16 1. We added a correlation map as you suggested and discussed the spatial structure of
17 climate-growth relationship (Fig. 4).

18

19 2. We discussed the issue over the instrumental period.

20

21 3. Indeed to compare our reconstruction to longer instrumental records from eastern
22 Mediterranean region, we visually compare and correlate with the European temperature
23 reconstruction by Xoplaki et al. 2005 to validate prior to 1930. This gridded
24 reconstruction gave the higher correlation than the other gridded reconstructions (which
25 you suggested in comment 4) over Turkey. We used the mean of corresponding grid
26 points from European spring temperature reconstruction over the study area (36–42° N,
27 26–38° E) to show how the correlation changed over past 200 years. We found significant
28 correlation (0.35, $p < 0.10$) for the period of 1901–1929 which climatic records are very
29 few over the region while available data has sufficient quality for most part of Europe
30 (Fig. 10).

31

32 4. We compared our tree-ring based temperature reconstruction with existing gridded
33 temperature reconstructions for Europe (Xoplaki et al. 2005, Luterbacher et al. 2016) and
34 the Old World Drought Atlas (OWDA) (Cook et al. 2015) (Figure 9a, b, c). We also
35 compared the precipitation signal (PC1) obtained from our tree-ring network with Old
36 World Drought Atlas (OWDA) (Cook et al. 2015) and gridded European summer
37 precipitation reconstruction (Pauling et al., 2006) to test the strength of the signal
38 spatially (Fig. 9d and e).

39

40 5. We added a review from suggested papers to Introduction.

41

42 Minor comments:

43

44

45 We cited Cook et al. 2015

46

47 We changed “the Medieval Climate Anomaly” to “the end of the Medieval Climate Anomaly”.

48

49

50 We deleted “Great Depression”.

51

52 We added “high resolution” to explain sensitivity of the gridded instrumental temperature.

53

54

55

56

57

58

59

60

61

62

63

64

65

66

67

68

69

70 **Spring temperature variability over Turkey since 1800 CE reconstructed**
71 **from a broad network of tree-ring data**

72

73 **Nesibe Köse^{(1),*}, H. Tuncay Güner⁽¹⁾, Grant L. Harley⁽²⁾, Joel Guiot⁽³⁾**

74

75 ⁽¹⁾Istanbul University, Faculty of Forestry, Forest Botany Department 34473 Bahçeköy-Istanbul,
76 Turkey

77 ⁽²⁾University of Southern Mississippi, Department of Geography and Geology, 118 College
78 Drive Box 5051, Hattiesburg, Mississippi, 39406, USA

79 ⁽³⁾ Aix-Marseille Université, CNRS, IRD, CEREGE UM34, ECCOREV, 13545 Aix-en-
80 Provence, France

81

82

83

84

85

86 *Corresponding author. Fax: +90 212 226 11 13

87 E-mail address: nesibe@istanbul.edu.tr

88

89 **Abstract**

90 The 20th century was marked by significant decreases in spring temperature ranges and increased
91 nighttime temperatures throughout Turkey. The meteorological observational period in Turkey,
92 which starts *ca.* 1929 CE, is too short for understanding long-term climatic variability. Hence,
93 the historical context of this gradual warming trend in spring temperatures is unclear. Here we
94 use a network of 23 tree-ring chronologies to provide a high-resolution spring (March–April)
95 temperature reconstruction over Turkey during the period 1800–2002. The reconstruction model
96 accounted for 67% (Adj. $R^2 = 0.64$, $p \leq 0.0001$) of the instrumental temperature variance over
97 the full calibration period (1930–2002). During the pre-instrumental period (1800–1929) we
98 captured more cold events ($n = 23$) than warm ($n = 13$), and extreme cold and warm events were
99 typically of short duration (1–2 years). Compared to coeval reconstructions of precipitation in the
100 region, our results are similar with durations of extreme wet and dry events. The reconstruction
101 is punctuated by a temperature increase during the 20th century; yet extreme cold and warm
102 events during the 19th century seem to eclipse conditions during the 20th century. During the 19th
103 century, annual temperature ranges are more volatile and characterized by more short-term
104 fluctuations compared to the 20th century. During the period 1900–2002, our reconstruction
105 shows a gradual warming trend, which includes the period during which diurnal temperature
106 ranges decreased as a result of increased urbanization in Turkey. [Comparisons with instrumental
107 gridded data and spatial climate reconstructions offered independent validation of this study and
108 revealed the potential for reconstructing temperature in an unlikely area, especially given the
109 strong precipitation signals displayed by most tree species growing in the dry Mediterranean
110 climate.](#)

112

113 KEYWORDS: Dendroclimatology, Climate reconstruction, *Pinus nigra*, Principle component

114 analysis, Spring temperature.

115 **1 Introduction**

116

117 Significant decreases in spring diurnal temperature ranges (DTR) occurred throughout Turkey
118 from 1929 to 1999 (Turkes & Sumer 2004). This decrease in spring DTRs was characterized by
119 day-time temperatures that remained relatively constant while a significant increase in night-time
120 temperatures were recorded over western Turkey and were concentrated around urbanized and
121 rapidly-urbanizing cities. The historical context of this gradual warming trend in spring
122 temperatures is unclear as the high-quality meteorological records in Turkey, which start in
123 1930~~29~~, are relatively short for understanding long-term climatic variability.

124

125 [An extensive body of literature details climate changes in the Mediterranean region over the last](#)
126 [two millennia \(c.f. Lionello, P. \(Ed.\), 2012\). Paleolimnological studies provide evidence that the](#)
127 [Medieval Climatic Anomaly \(MCA; 900–1300 CE\) characterized warm and dry conditions over](#)
128 [the Iberian Peninsula, while the Little Ice Age \(LIA; 1300–1850 CE\) brought opposite climate](#)
129 [conditions, forced by interactions between the East Atlantic and North Atlantic Oscillation](#)
130 [\(Sanchez-Lopez et al. 2016\). In addition, Roberts et al. \(2012\) highlighted an intriguing spatial](#)
131 [dipole NAO pattern between the western and eastern Mediterranean region, which brought anti-](#)
132 [phased warm \(cool\) and wet \(dry\) conditions during the MCA and LIA. The hydro-climate](#)
133 [patterns revealed by previous investigations appear to have been forced not only by NAO, but](#)
134 [other climate modes with non-stationary teleconnections across the region \(Roberts et al. 2012\).](#)

135

136 Tree rings have shown to provide useful information about the past climate of Turkey and were
137 used intensively during the last decade to reconstruct precipitation in the Aegean (Griggs et al.

138 2007), Black Sea (Akkemik et al. 2005, 2008; Martin-Benitto et al. 2016), Mediterranean regions
139 (Touchan et al. 2005a), as well as the Sivas (D'Arrigo & Cullen 2001), southwestern (Touchan et
140 al. 2003, Touchan et al. 2007; Köse et al. 2013), south-central (Akkemik & Aras 2005) and
141 western Anatolian (Köse et al. 2011) regions of Turkey. These studies used tree rings to
142 reconstruct precipitation because available moisture is often found to be the most important
143 limiting factor that influences radial growth of many tree species in Turkey. These studies
144 revealed past spring-summer precipitation, and described past dry and wet events and their
145 duration. Recently, [Cook et al. \(2015\) presented Old World Drought Atlas \(OWDA\), which is a](#)
146 [set of year by year maps of reconstructed Palmer Drought Severity Index from tree-ring](#)
147 [chronologies over the Europe and Mediterranean Basin.](#) Heinrich et al. (2013) provided a winter-
148 to-spring temperature proxy for Turkey from carbon isotopes within the growth rings of
149 *Juniperus excelsa* since AD 1125. Low-frequency temperature trends corresponding to the [end](#)
150 [of](#) Medieval Climatic Anomaly and Little Ice Age were identified in the record, but the proxy
151 failed to identify the recent warming trend during the 20th century. In this study, we present a
152 tree-ring based spring temperature reconstruction from Turkey and compare our results to
153 previous reconstructions of temperature and precipitation to provide a more comprehensive
154 understanding of climate conditions during the 19th and 20th centuries.

155

156 **2 Data and Methods**

157 2.1 Climate of the Study Area

158

159 The study area, which spans 36–42° N and 26–38° E, was based on the distribution of available
160 tree-ring chronologies. This vast area covers much of western Anatolia and includes the western

161 Black Sea, Marmara, and western Mediterranean regions. Much of this area is characterized by a
162 Mediterranean climate that is primarily controlled by polar and tropical air masses (Türkeş
163 1996a, Deniz et al. 2011). In winter, polar fronts from the Balkan Peninsula bring cold air that is
164 centered in the Mediterranean. Conversely, the dry, warm conditions in summer are dominated
165 by weak frontal systems and maritime effects. Moreover, the Azores high-pressure system in
166 summer and anticyclonic activity from the Siberian high-pressure system often cause below
167 normal precipitation and dry sub-humid conditions over the region (Türkeş 1999, Deniz et al.
168 2011). In this Mediterranean climate, annual mean temperature and precipitation range from 3.6
169 °C to 20.1 °C and from 295 to 2220 mm, respectively, both of which are strongly controlled by
170 elevation (Deniz et al. 2011).

171

172 2.2 Development of tree-ring chronologies

173

174 To investigate past temperature conditions, we used a network of 23 tree-ring site chronologies
175 (Fig. 1). Fifteen chronologies were produced by previous investigations (Mutlu et al. 2011,
176 Akkemik et al. 2008, Köse et al. unpublished data, Köse et al. 2011, Köse et al. 2005) that
177 focused on reconstructing precipitation in the study area. In addition, we sampled eight new
178 study sites and developed tree-ring time series for these areas (Table 1). Increment cores were
179 taken from living *Pinus nigra* Arn. and *Pinus sylvestris* L. trees and cross-sections were taken
180 from *Abies nordmanniana* (Steven) Spach and *Picea orientalis* (L.) Link trunks.

181

182 Samples were processed using standard dendrochronological techniques (Stokes & Smiley 1968,
183 Orvis & Grissino-Mayer 2002, Speer 2010). Tree-ring widths were measured, then visually

184 crossdated using the list method (Yamaguchi 1991). We used the computer program COFECHA,
185 which uses segmented time-series correlation techniques, to statistically confirm our visual
186 crossdating (Holmes 1983, Grissino-Mayer 2001). Crossdated tree-ring time series were then
187 standardized by fitting a 67% cubic smoothing spline with a 50% cutoff frequency to remove
188 non-climatic trends related to the age, size, and the effects of stand dynamics using the ARSTAN
189 program (Cook 1985, Cook et al. 1990a). These detrended series were then pre-whitened with
190 low-order autoregressive models to produce time series with a strong common signal and
191 without biological persistence. These series may be more suitable to understand the effect of
192 climate on tree-growth, even if any persistence due to climate might be removed by pre-
193 whitening. For each chronology, the individual series were averaged to a single chronology by
194 computing the biweight robust means to reduce the influences of outliers (Cook et al. 1990b). In
195 this research we used residual chronologies obtained from ARSTAN to reconstruct temperature.

196

197 The mean sensitivity, which is a metric representing the year-to-year variation in ring width
198 (Fritts 1976), was calculated for each chronology and compared. The minimum sample depth for
199 each chronology was determined according to expressed population signal (EPS), which we used
200 as a guide for assessing the likely loss of reconstruction accuracy. Although arbitrary, we
201 required the commonly considered threshold of $EPS > 0.85$ (Wigley et al. 1984; Briffa & Jones
202 1990).

203

204 2.3 ~~Temperature reconstruction~~Identifying relationship between tree-ring width and climate

205

206 We extracted high resolution monthly temperature and precipitation records from the climate
207 dataset CRU TS 3.23 gridded at 0.5° intervals (Jones and Harris 2008) from KNMI Climate
208 Explorer (<http://climexp.knmi.nl>) for 36–42 °N, 26–38 °E. The period AD 1930–2002 was
209 chosen for the analysis because it maximized the number of station records within the study area.

210

211 First, the climate-growth relationships were investigated with response function analysis (RFA)
212 (Fritts 1976) for biological year from previous October to current October using the

213 DENDROCLIM2002 program (Biondi & Waikul 2004). This analysis is done to determine the

214 months during which the tree-growth is the most responsive to temperature. RFA results showed

215 that precipitation from May to August and temperature in March and April have dominant

216 control on tree-ring formation in the area. Second, we produced correlation maps showing

217 correlation coefficients between tree-ring chronologies and the ~~most important~~ climate factors

218 most important for tree growth, which are ~~May to~~ August precipitation and ~~March to~~ April

219 temperature, to find the spatial structure of radial growth–climate relationship (St. George 2014,

220 St. George and Ault 2014, Hellmann et al. 2016). For each site we used the closest gridded

221 temperature and precipitation values.

222

223 2.4 Temperature reconstruction

224

225 The climate reconstruction is performed by regression based on the principal component (PCs)

226 of the 23 chronologies within the study area. Principle Component Analysis (PCA) was done

227 over the entire period in common to the tree-ring chronologies. The significant PCs were

228 selected by stepwise regression. We combined forward selection with backward elimination

229 setting $p \leq 0.05$ as entrance tolerance and $p \leq 0.1$ as exit tolerance. The final model obtained when
230 the regression reaches a local minimum of RMSE. The order of entry of the PCs into the model
231 was PC₃, PC₂₁, PC₄, PC₁₅, PC₅, PC₁₇, PC₇, PC₉, PC₁₀. The regression equation is calibrated on
232 the common period (1930–2002) between robust temperature time-series and the selected tree-
233 ring series. Third, the final reconstruction is based on bootstrap regression (Till and Guiot, 1990),
234 a method designed to calculate appropriate confidence intervals for reconstructed values and
235 explained variance even in cases of short time-series. It consists in randomly resampling the
236 calibration datasets to produce 1000 calibration equations based on a number of slightly different
237 datasets.

238 The quality of the reconstruction is assessed by a number of standard statistics. The overall
239 quality of fit of reconstruction is evaluated based on the determination coefficient (R^2), which
240 expresses the percentage of variance explained by the model and the root mean squared error
241 (RMSE), which expresses the calibration error. This does not insure the quality of the
242 extrapolation which needs additional statistics based on independent observations, i.e.
243 observations not used by the calibration (verification data). They are provided by the
244 observations not resampled by the bootstrap process. The prediction RMSE (called RMSEP), the
245 reduction of error (RE) and the coefficient of efficiency (CE) are calculated on the verification
246 data and enable to test the predictive quality of the calibrated equations (Cook et al, 1994).

247 Traditionally, a positive RE or CE values means a statistically significant reconstruction model,
248 but bootstrap has the advantage to produce confidence intervals for such statistics without
249 theoretical probability distribution and finally we accept the RE and CE for which the lower
250 confidence margin at 95% are positive. This is more constraining than just accepting all positive

251 RE and CE. For additional verification, we also present traditional split-sample procedure results
252 that divided the full period into two subsets of equal length (*Meko and Graybill, 1995*).

253
254 To identify the extreme March–April cold and warm events in the reconstruction, standard
255 deviation (SD) values were used. Years one and two SD above and below the mean were
256 identified as warm, very warm, cold, and very cold years, respectively. ~~Finally, as~~ As a way to
257 assess the spatial representation of our temperature reconstruction, we conducted a spatial field
258 correlation analysis between reconstructed values and the gridded CRU TS3.23 temperature field
259 (Jones and Harris 2008) for a broad region of the Mediterranean over the entire instrumental
260 period (ca. 1930–2002). Finally, we compared our temperature reconstruction and also
261 precipitation signal (PC1) against existing gridded temperature and hydroclimate reconstructions
262 for Europe over the period 1800–2002. We performed spatial correlation analysis : ~~1)~~ between
263 [1] our temperature reconstruction, and gridded temperature reconstructions for Europe (Xoplaki
264 et al. 2005, Luterbacher et al. 2016) and OWDA (Cook et al. 2015); and [2] 2) between-PC1 and
265 summer precipitation reconstruction (Pauling et al., 2006) and OWDA (Cook et al. 2015).

266

267 **2 Results and Discussion**

268 2.1 Tree-ring chronologies

269 In addition to 15 chronologies developed by previous studies, we produced six *P. nigra*, one *P.*
270 *sylvestris*, one *A. nordmanniana* / *P. orientalis* chronologies for this study (Table 2). The Çorum
271 district produced two *P. nigra* chronologies: one the longest (KAR; 627 years long) and the other
272 the most sensitive to climate (SAH; mean sensitivity value of 0.25). Previous investigations of
273 climate-tree growth relationships reported a mean sensitivity range of 0.13–0.25 for *P. nigra* in

274 Turkey (Köse 2011, Akkemik et al. 2008). The KAR, SAH, and ERC chronologies (with mean
275 sensitivity values from 0.22 to 0.25) were classified as very sensitive, and the SAV, HCR, and
276 PAY chronologies (mean sensitivity values range 0.17–0.18) contained values characteristic of
277 being sensitive to climate. The lowest mean sensitivity value was obtained for the ART A.
278 *nordmanniana* / *P. orientalis* chronology. Nonetheless, this chronology retained a statistically
279 significant temperature signal ($p < 0.05$).

280

281 2.2 ~~March–April temperature reconstruction~~ Tree-ring growth-climate relationship

282 RFA coefficients of May to August precipitation are positively correlated with most of the tree-
283 ring series (Fig. 2) and among them, May and June coefficients are generally significant. The
284 first principal component of the 23 chronologies, which explains 47% of the tree-growth
285 variance, is highly correlated with May–August total precipitation, statistically ($r = 0.65$, $p \leq$
286 0.001) and visually (Fig. 3). The high correlation was expected given that numerous studies also
287 found similar results in Turkey (Akkemik 2000a, Akkemik 2000b, Akkemik 2003, Akkemik et
288 al. 2005, Akkemik et al. 2008, Akkemik & Aras 2005, Hughes et al. 2001, D'Arrigo & Cullen
289 2001, Touchan et al. 2003; Touchan et al. 2005a, Touchan et al. 2005b, Touchan et al. 2007,
290 Köse et al. 2011, Köse et al. 2012, Köse et al. 2013, Martin-Benitto et al. 2016). The influence of
291 temperature was not as strong as May–August precipitation on radial growth, although generally
292 positive in early spring (March and April) (Fig. 2). Conversely, the ART chronology from
293 northeastern Turkey contained a strong temperature signal, which was significantly positive in
294 March. ~~In addition to this chronology, we also used the chronologies that revealed the influence~~
295 ~~of precipitation, as well as temperature to reconstruct March–April temperature.~~

296

297
298 Correlation maps representing influence of May-August precipitation (Fig. 4a) and March-April
299 temperature (Fig 4b) also showed that strength of the summer precipitation signal is higher and
300 significant almost all over the Turkey. Higher precipitation in summer has a positive effect on
301 tree-growth, because of long-lasting dry and warm conditions over the Turkey (Türkeş 1996b,
302 Köse et al. 2012). Spring precipitation signal are generally positive and significant only for four
303 tree-ring sites. The sites located at the upper distributions of the species are generally showed
304 higher correlations. The highest correlations obtained for *Picea/Abies* chronology (ART) from
305 the Caucasus, and for *Pinus nigra* chronology (HCR) from the upper (about 1900 m) and
306 southeastern distribution of the species. This black pine forest was still partly covered by snow
307 from previous year during the field work in fall. Higher temperatures in spring maybe cause
308 snow melt earlier and lead to produce larger annual rings. ~~In addition to this~~ these chronologies.
309 we also used the chronologies that revealed the influence of precipitation, as well as temperature
310 to reconstruct March–April temperature.

311
312

313 2.3 March-April temperature reconstruction

314 The higher order PCs of the 23 chronologies are significantly correlated with the March–April
315 temperature and, by nature, are independent on the precipitation signal (Table 3). The best
316 selection for fit temperature are obtained with the PC₃, PC₄, PC₅, PC₇, PC₉, PC₁₀, PC₁₅, PC₁₇,
317 PC₂₁, which explains together 25% of the tree-ring chronologies. So the temperature signal
318 remains important in the tree-ring chronologies and can be reconstructed. The advantage to
319 separate both signals through orthogonal PCs enable to remove an unwanted noise for our

320 temperature reconstruction. Thus, PC₁ was not used as potential predictor of temperature because
321 it is largely dominated by precipitation (Table 3, Fig. 3). The last two PCs contain a too small
322 part of the total variance to be used in the regressions. However, even if Jolliffe (1982) and Hadi
323 & Ling (1998) claimed that certain PCs with small eigenvalues (even the last one), which are
324 commonly ignored by principal components regression methodology, may be related to the
325 independent variable, we must be cautious with that because they may be much more dominated
326 by noise than the first ones. So, the contribution of each PC to the regression sum of squares is
327 also important for selection of PCs (Hadi & Ling 1998). The findings of Jolliffe (1982) and Hadi
328 & Ling (1998) provide a justification for using non-primary PCs, (*e.g.*, of second and higher
329 order) in our regression, given that correlations with temperature may be over-powered by
330 affects from precipitation in our study area (Cook 2011, personal communication).

331
332 Using this method, the calibration and verification statistics indicated a statistically significant
333 reconstruction (Table 4, Fig. 54). For additional verification, we also present split-sample
334 procedure results. Similarly bootstrap results, the derived calibration and verification tests using
335 this method indicated a statistically significant RE and CE values (Table 5).

336
337 The regression model accounted for 67% (Adj. $R^2 = 0.64$, $p \leq 0.0001$) of the actual
338 temperature variance over the calibration period (1930–2002). Also, actual and reconstructed
339 March–April temperature values had nearly identical trends during the period 1930–2002 (Fig.
340 54). Moreover, the tree-ring chronologies successfully simulated both high frequency and
341 warming trends in the temperature data during this period. The reconstruction was more
342 powerful at classifying warm events rather than cold events. Over the last 73 years, eight of ten

343 warm events in the instrumental data were also observed in the reconstruction, while five of nine
344 cold events were captured. Similarly, previous tree-ring based precipitation reconstructions for
345 Turkey (Köse et al. 2011; Akkemik et al. 2008) were generally more successful in capturing dry
346 years rather than wet years.

347
348 Our temperature reconstruction on the 1800–2002 period is obtained by bootstrap regression,
349 using 1000 iterations (Fig. 65). The confidence intervals are obtained from the range between the
350 2.5th and the 97.5th percentiles of the 1000 simulations. For the pre-instrumental period (1800–
351 1929), a total of 23 cold (1813, 1818, 1821, 1824, 1837, 1848, 1854, 1858, 1860, 1869, 1877–
352 1878, 1880–1881, 1883, 1897–1898, 1905–1907, 1911–1912, 1923) and 13 warm (1801–1802,
353 1807, 1845, 1853, 1866, 1872–1873, 1879, 1885, 1890, 1901, 1926) events were determined.
354 After comparing our results with event years obtained from May–June precipitation
355 reconstructions from western Anatolia (Köse et al. 2011), the cold years 1818, 1848, and 1897
356 appeared to coincide with wet years and 1881 was a very wet year for the entire region.
357 Furthermore, these years can be described as cold (in March–April) and wet (in May–June) for
358 western Anatolia.

359
~~360 Spatial correlation analysis revealed that our network-based temperature reconstruction was~~
~~361 representative of conditions across Turkey, as well as the broader Mediterranean region (Fig. 6).~~
~~362 During the period 1930–2002, estimated temperature values were highly significant (r range 0.5–~~
~~363 0.6, $p < 0.01$) with instrumental conditions recorded from southern Ukraine to the west across~~
~~364 Romania, and from northern areas of Libya and Egypt to the east across Iraq. The strength of the~~
~~365 reconstruction model is evident in the broad spatial implications demonstrated by the~~

366 ~~temperature record. Thus, we interpret warm and cold periods and extreme events within the~~
367 ~~record with high confidence.~~

368
369 Among the warm periods in our reconstruction, conditions during the year 1879 were dry, 1895
370 wet, and 1901 very wet across the broad region of western Anatolia (Köse et al. 2011). Hence,
371 we defined 1879 as a warm (in March–April) and dry year (in May–June), and 1895 and 1901
372 were warm and wet years. In the years 1895 and 1901 the combination of a warm early spring
373 and a wet late spring-summer caused enhanced radial growth in Turkey, interpreted as longer
374 growing seasons without drought stress.

375
376 Of these event years, 1897 and 1898 were exceptionally cold and 1845, 1872 and 1873 were
377 exceptionally warm. During the last 200 years, our reconstruction suggests that the coldest year
378 was 1898 and the warmest year was 1873. The reconstructed extreme events also coincided with
379 accounts from historical records. Server (2008) recounted the winter of 1898 as characterized by
380 anomalously cold temperatures that persisted late into the spring season. A family, who brought
381 their livestock herds up into the plateau region in Kırşehir seeking food and water were suddenly
382 covered in snow on 11 March 1898. This account of a late spring freeze supports the
383 reconstruction record of spring temperatures across Turkey, and offers corroboration to the
384 quality of the reconstructed values.

385
386 Seyf (1985) reported that extreme summer temperature during the year 1873 resulted in
387 widespread crop failure and famine. Historical documents recorded an infamous drought-derived
388 famine that occurred in Anatolia from 1873 to 1874 (Quataert, 1996, Kuniholm, 1990), which

389 claimed the lives of 250,000 people and a large number of cattle and sheep (Faroghi, 2009). This
390 drought caused widespread mortality of livestock and depopulation of rural areas through human
391 mortality, and migration of people from rural to urban areas. Further, the German traveler
392 Naumann (1893) reported a very dry and hot summer in Turkey during the year 1873 (Heinrich
393 et al, 2013). Conditions worsened when the international stock exchanges crashed in 1873;
394 ~~marking the beginning of the "Great Depression" in the European economy~~ (Zürcher, 2004). Our
395 temperature record suggests that dry conditions during the early 1870s were possibly exacerbated
396 by warm spring temperatures that likely carried into summer. A similar pattern of intensified
397 drought by warm temperatures was demonstrated recently by Griffin and Anchukaitis (2014) for
398 the current drought in California, USA.

399
400 Extreme cold and warm events were usually one year long, and the longest extreme cold and
401 warm events were two and three years, respectively. These results were similar with durations of
402 extreme wet and dry events in Turkey (Touchan et al. 2003, Touchan et al. 2005a, Touchan et al.
403 2005b, Touchan et al. 2007, Akkemik & Aras, 2005, Akkemik et al. 2005, Akkemik et al. 2008,
404 Köse et al. 2011). Moreover, seemingly innocuous short-term warm events, such as the 1807
405 event, were recorded across the Mediterranean and in high elevations of the European regions.
406 Casty et al. (2005) reported the year 1807 as being one of the warmest alpine summers in the
407 European Alps over the last 500 years. As such, a drought record from Nicault et al. (2008)
408 echoes this finding, as a broad region of the Mediterranean basin experienced drought
409 conditions.

410

411 Low frequency variability of our spring temperature reconstruction showed larger variability in
412 nineteenth century than twentieth century. Similar results observed on previous tree-ring based
413 precipitation reconstructions from Turkey (Touchan et al. 2003, D'Arrigo et al. 2001, Akkemik
414 and Aras 2005, Akkemik et al. 2005, Köse et al. 2011). Moreover, cold (warm) periods observed
415 in our reconstruction are generally appeared as generally wet in the precipitation reconstructions,
416 while ~~warm periods generally~~rarely -correlated with dry (wet) periods (Fig. 77). When we
417 compare the relationship between temperature and precipitation over the instrumental period
418 both case, cold (warm) and wet (dry) as well as cold (warm) and dry (wet), can be observed.

419
420 Heinrich et al. (2013) analyzed winter-to-spring (January–May) air temperature variability in
421 Turkey since AD 1125 as revealed from a robust tree-ring carbon isotope record from *Juniperus*
422 *excelsa*. Although they offered a long-term perspective of temperature over Turkey, the
423 reconstruction model, which covered the period 1949–2006, explained 27% of the variance in
424 temperature since the year 1949. In this study, we provided a short-term perspective of
425 temperature fluctuation based on a robust model (calibrated and verified 1930–2002; Adj. $R^2 =$
426 0.64; $p \leq 0.0001$). Yet, the Heinrich et al. (2013) temperature record did not capture the 20th
427 century warming trend as found elsewhere (Wahl et al. 2010). However, their temperature trend
428 does agree with trend analyses conducted on meteorological data from Turkey and other areas in
429 the eastern Mediterranean region. The warming trend seen during our reconstruction calibration
430 period (1930–2002) was similar to the data shown by Wahl et al. (2010) across the region and
431 hemisphere. Further, the warming trends seen in our record agrees with data presented by Turkes
432 & Sumer (2004), of which they attributed to increased urbanization in Turkey. Considering long-
433 term changes in spring temperatures, the 19th century was characterized by more high-frequency

434 fluctuations compared to the 20th century, which was defined by more gradual changes and
435 includes the beginning of decreased DTRs in the region (Turkes & Sumer, 2004).

436

437 4 Comparison with instrumental gridded data and spatial reconstructions

438

439 Spatial correlation analysis revealed that our network-based temperature reconstruction was
440 representative of conditions across Turkey, as well as the broader Mediterranean region (Fig. 8).
441 During the period 1930–2002, estimated temperature values were highly significant (r range 0.5–
442 0.6, $p < 0.01$) with instrumental conditions recorded from southern Ukraine to the west across
443 Romania, and from northern areas of Libya and Egypt to the east across Iraq. The strength of the
444 reconstruction model is evident in the broad spatial implications demonstrated by the
445 temperature record. Thus, we interpret warm and cold periods and extreme events within the
446 record with high confidence.

447

448 We compared our tree-ring based temperature reconstruction with existing gridded temperature
449 reconstructions for Europe (Xoplaki et al. 2005, Luterbacher et al. 2016) and the Old World
450 Drought Atlas (OWDA) (Cook et al. 2015) for further validation of the reconstruction (Figure
451 9a, b, c, respectively). Spatial correlations over the past 200 years were lower with reconstructed
452 European summer temperature (May to July) (Fig 9b). Yet, we expected this result because of
453 the paucity of Turkey-derived proxies in the other reconstructions, as well as the differing
454 seasons involved across the reconstructions. Similarly, our reconstruction showed weak
455 correlations with summer drought index over Turkey. Beside comparing different seasons,
456 perhaps this is because less precipitation begets drought conditions rather than high temperature

457 in the region. The highest and significant ($p < 0.01$) correlations were found with European
458 spring (March to May) temperature reconstruction over Turkey (Fig 9a). We used the mean of
459 corresponding grid points from European spring temperature reconstruction over the study area
460 (36–42° N, 26–38° E) to show how the correlation changed over time (Figure 10). The
461 correlation coefficient was highly significant (0.76, $p < 0.001$) during our calibration period
462 (1930–2002). We found lower but still significant correlation (0.35, $p < 0.10$) for the period of
463 1901–1929, which climatic records are very few over the region while available data has
464 sufficient quality for most part of Europe. These results give additional verification for our
465 reconstruction. Moreover, our reconstruction has a weak, insignificant relationship (0.13, $p >$
466 0.10) during the 19th century. This may be related to poor reconstructive skill of European spring
467 temperature reconstruction over Turkey, which contains few proxies from the country (Xoplaki
468 et al. 2005, Luterbacher et al. 2004). Nonetheless, these results demonstrate that tree-ring
469 chronologies from Turkey can serve as useful temperature proxies for further spatial temperature
470 reconstructions to fill the gaps in the area.

471
472 We also compared the precipitation signal (PC1) obtained from our tree-ring network with Old
473 World Drought Atlas (OWDA) (Cook et al. 2015) and gridded European summer precipitation
474 reconstruction (Pauling et al., 2006) to test the strength of the signal spatially (Fig. 9d and e,
475 respectively). We found positive but not so strong correlations over Turkey with European
476 summer precipitation reconstruction. Pauling et al. (2006) stated that poor reconstructive skills
477 determined over Turkey because of few instrumental record before the 1930s. We calculated
478 highly significant correlations with summer drought index over Turkey and neighboring
479 European countries such as Greece, Bulgaria, and Romania. These results showed that summer

480 precipitation signal represented by PC1 is very strong not only on instrumental period, but also
481 on pre-instrumental period, and represents a large spatial coverage.

482

483

484 **4 Conclusions**

485

486 In this study, we used a broad network of tree-ring chronologies to provide the first tree-ring
487 based temperature reconstruction for Turkey and identified extreme cold and warm events during
488 the period 1800–1929 CE. Similar to the precipitation reconstructions against which we compare
489 our air temperature record, extreme cold and warm years were generally short in duration (one
490 year) and rarely exceeded two-three years in duration. The coldest and warmest years over
491 western Anatolia were experienced during the 19th century, and the 20th century is marked by a
492 temperature increase.

493

494 Reconstructed temperatures for the 19th century suggest that more short-term fluctuations
495 occurred compared to the 20th century. The gradual warming trend shown by our reconstruction
496 calibration period (1930–2002) is coeval with decreases in spring DTRs. Given the results of
497 Turkes and Sumer (2004), the variations in short- and long-term temperature changes between
498 the 19th and 20th centuries might be related to increased urbanization in Turkey.

499

500 The study revealed the potential for reconstructing temperature in an area previously thought
501 impossible, especially given the strong precipitation signals displayed by most tree species
502 growing in the dry Mediterranean climate that characterizes broad areas of Turkey. Our

503 reconstruction only spans 205 years due to the shortness of the common interval for the
504 chronologies used in this study, but the possibility exists to extend our temperature
505 reconstruction further back in time by increasing the sample depth with more temperature-
506 sensitive trees, especially from northeastern Turkey. Thus future research will focus on
507 increasing the number of tree-ring sites across Turkey, and maximizing chronology length at
508 existing sites that would ultimately extend the reconstruction back in time.

509

510 **Acknowledgements**

511

512 This research was supported by The Scientific and Technical Research Council of Turkey
513 (TUBITAK); Projects ÇAYDAG 107Y267 and YDABAG 102Y063. N. Köse was supported by
514 The Council of Higher Education of Turkey. We are grateful to the Turkish Forest Service
515 personnel and Ali Kaya, Umut Ç. Kahraman and Hüseyin Yurtseven for their invaluable support
516 during our field studies. [We thank to Dr. Ufuk Turuncoğlu for his help on spatial analysis.](#) J.
517 Guiot was supported by the Labex OT-Med (ANR-11-LABEX-0061), French National Research
518 Agency (ANR).

519

520 **References**

- 521 Akkemik, Ü.: Dendroclimatology of Umbrella pine (*Pinus pinea* L.) in Istanbul (Turkey), Tree-
522 Ring Bull., 56, 17–20, 2000a.
- 523 Akkemik, Ü.: Tree-ring chronology of *Abies cilicica* Carr. in the Western Mediterranean Region
524 of Turkey and its response to climate, Dendrochronologia, 18, 73–81, 2000b.
- 525 Akkemik, Ü.: Tree-rings of *Cedrus libani* A. Rich the northern boundary of its natural
526 distribution, IAWA J, 24(1), 63-73, 2003.
- 527 Akkemik, Ü. and Aras, A.: Reconstruction (1689–1994) of April–August precipitation in
528 southwestern part of central Turkey, Int. J. Clim., 25, 537–548, 2005.
- 529 Akkemik, Ü., Dagdeviren, N., and Aras, A.: A preliminary reconstruction (A.D. 1635–2000) of
530 spring precipitation using oak tree rings in the western Black Sea region of Turkey, Int. J.
531 Biomet., 49(5), 297–302, 2005.
- 532 Akkemik, Ü., D’Arrigo, R., Cherubini, P., Köse, N., and Jacoby, G.: Tree-ring reconstructions of
533 precipitation and streamflow for north-western Turkey, Int. J. Clim., 28, 173–183, 2008.
- 534 Biondi, F. and Waikul, K.: DENDROCLIM2002: A C++ program for statistical calibration of
535 climate signals in tree-ring chronologies, Comp. Geosci., 30, 303–311, 2004.
- 536 Briffa, K. R. and Jones, P. D.: Basic chronology statistics and assessment. In: Methods of
537 Dendrochronology: Applications in the Environmental Sciences (Cook, E. and Kairiukstis, L.
538 A. eds). Kluwer Academic Publishers, Amsterdam, pp. 137–152, 1990.
- 539 Casty, C., Wanner, H., Luterbacher, J., Esper, J., and Böhm, R.: Temperature and precipitation
540 variability in the European Alps since 1500, Int. J. Clim., 25(14), 1855–1880, 2005.

541 Cook, E.: A time series analysis approach to tree-ring standardization. PhD. Dissertation.
542 University of Arizona, Tucson, 1985.

543 Cook, E., Briffa, K., Shiyatov, S., and Mazepa, V.: Tree-ring standardization and growth-trend
544 estimation. In: *Methods of Dendrochronology: Applications in the Environmental Sciences*
545 (Cook, E. and Kairiukstis, L. A. eds). Kluwer Academic Publishers, Amsterdam, pp.104–
546 122, 1990a.

547 Cook, E., Shiyatov, S., and Mazepa, V.: Estimation of the mean chronology. In: *Methods of*
548 *Dendrochronology: Applications in the Environmental Sciences* (Cook, E. and Kairiukstis, L.
549 A. eds). Kluwer Academic Publishers, Amsterdam, pp. 123–132, 1990b.

550 [Cook, E.R, Seager R., et al.: Old World megadroughts and pluvials during the Common Era. *Sci.*](#)
551 [*Adv.*, 1, e1500561, doi:10.1126/sciadv.1500561, 2015.](#)

552 D'Arrigo, R. and Cullen, H. M.: A 350-year (AD 1628–1980) reconstruction of Turkish
553 precipitation. *Dendrochronologia* ,19(2), 169–177, 2001.

554 Deniz, A., Toros, T., and Incecik, S.: Spatial variations of climate indices in Turkey, *Int. J.*
555 *Clim.*, 31, 394-403, 2011.

556 Fritts, H. C.: *Tree Rings and Climate*. Academic Press, New York, 1976.

557 Griggs, C., DeGaetano, A., Kuniholm, P., and Newton, M.: A regional high-frequency
558 reconstruction of May–June precipitation in the north Aegean from oak tree rings, A.D.
559 1809–1989, *Int. J. Clim.*, 27, 1075–1089, 2007.

560 Grissino-Mayer, H. D.: Evaluating crossdating accuracy: A manual and tutorial for the computer
561 program COFECHA, *Tree-Ring Res.*, 57, 205–221, 2001.

562 Griffin, D. and Anchukaitis, K. J.: How unusual is the 2012–2014 California drought? *Geophys.*
563 *Res. Lett.*, 41(24), 9017–9023, 2014.

564 Hadi, A. S. and Ling, R. F.: Some cautionary notes on the use of principal components
565 regression, *Amer. Statist.*, 52(1), 15–19, 1998.

566 Heinrich, I., Touchan, R., Liñán, I. D., Vos, H., and Helle, G.: Winter-to-spring temperature
567 dynamics in Turkey derived from tree rings since AD 1125, *Clim. Dynam.*, 41(7–8), 1685–
568 1701, 2013.

569 [Hellmann, L., Agafonov, L., et al.: Diverse growth trends and climate responses across Eurasia's
570 boreal forest. *Environmental Research Letters*: 11: 074021, doi:10.1088/1748-
571 9326/11/7/074021.](#)

572 Holmes, R. L.: Computer-assisted quality control in tree-ring data and measurements, *Tree-Ring*
573 *Bull.*, 43, 69–78, 1983.

574 Hughes, M. K., Kuniholm, P. I., Garfin, G. M., Latini, C., and Eischeid, J.: Aegean tree-ring
575 signature years explained, *Tree-Ring Res.*, 57(1), 67–73, 2001.

576 Jolliffe, I. T.: A note on the use of principal components in regression, *Appl. Stat.*, 31(3), 300–
577 303, 1982.

578 Jones, P. D. and Harris, I.: Climatic Research Unit (CRU) time-series datasets of variations in
579 climate with variations in other phenomena. NCAS British Atmospheric Data Centre, 2008.
580 <http://catalogue.ceda.ac.uk/uuid/3f8944800cc48e1cbc29a5ee12d8542d>

581 Köse, N., Akkemik, Ü., and Dalfes, H. N.: Anadolu'nun iklim tarihinin son 500 yılı:
582 Dendroklimatolojik ilk sonuçlar. Türkiye Kuvaterner Sempozyumu-TURQUA-V, 02–03
583 Haziran 2005, *Bildiriler Kitabı*, 136–142 (In Turkish), 2005.

584 Köse, N., Akkemik, Ü., Dalfes, H. N., and Özeren, M. S.: Tree-ring reconstructions of May–June
585 precipitation of western Anatolia, *Quat. Res.*, 75, 438–450, 2011.

586 [Köse, N., Akkemik, Ü., Dalfes, H. N., and Özeren, M. S., Tolunay D.: Tree-ring growth of *Pinus*
587 *nigra* Arn. subsp. *pallasiana* under different climate conditions throughout western Anatolia,
588 *Dendrochronologia*, 295-301, 2012.](#)

589 Köse, N., Akkemik, U., Guner, H.T., Dalfes, H.N., Grissino-Mayer, H.D., Ozeren, M.S., Kindap,
590 T.: An improved reconstruction of May– June precipitation using tree-ring data from western
591 Turkey and its links to volcanic eruptions, *Int. J. Biometeorol.*, 57(5), 691–701, 2013.

592 [Lionello, P. \(Ed.\): The Climate of the Mediterranean Region, from the Past to the Future.
593 Elsevier, Amsterdam, Netherlands, 2012.](#)

594 [Luterbacher, J., Dietrich, D., Xoplaki, E., Grosjean, M., Wanner, H.: European seasonal and
595 annual temperature variability, trends and extremes since 1500. *Science*, 303, 1499–1503,
596 2004.](#)

597 [Luterbacher, J., Werner, J.P., et al.: European summer temperatures since Roman times.
598 *Environmental Research Letters*, 11: 024001, doi:10.1088/1748-9326/11/1/024001, 2016.](#)

599 Martin-Benito, D., Ummenhofer C.C., Köse, N., Güner, H.T., Pederson, N.: ~~2016.~~ Tree-ring
600 reconstructed May-June precipitation in the Caucasus since 1752 CE, *Clim. Dyn.*, DOI
601 10.1007/s00382-016-3010-1, 2016.

602 Meko, D. M. and Graybill, D. A.: Tree-ring reconstruction of upper Gila River discharge, *Wat.*
603 *Res. Bull.*, 31, 605–616, 1995.

604 Mutlu, H., Köse, N., Akkemik, Ü., Aral, D., Kaya, A., Manning, S. W., Pearson, C. L., and
605 Dalfes, N.: Environmental and climatic signals from stable isotopes in Anatolian tree rings,
606 Turkey, *Reg. Environ. Change*, doi: 10.1007/s1011301102732, 2011.

607 Nicault, A., Alleaume, S., Brewer, S., Carrer, M., Nola, P., and Guiot, J.: Mediterranean drought
608 fluctuation during the last 500 years based on tree-ring data, *Clim. Dynam.*, 31(2–3), 227–
609 245, 2008.

610 Orvis, K. H. and Grissino-Mayer, H. D.: Standardizing the reporting of abrasive papers used to
611 surface tree-ring samples, *Tree-Ring Res.*, 58, 47–50, 2002.

612 [Pauling, A., Luterbacher, J., Casty, C., Wanner, H.: Five hundred years of gridded high-](#)
613 [resolution precipitation reconstructions over Europe and the connection to large-scale](#)
614 [circulation. *Clim. Dynam.*, 26, 387–405, 2006.](#)

615 [Roberts, N., Moreno, A., Valero-Garces, B.L.: Palaeolimnological evidence for an east-west](#)
616 [climate see-saw in the Mediterranean since AD 900. *Glob. Planet. Change*, 84, 23–34, 2012.](#)

617 [Sanchez-López, G. Hernandez, A., Pla-Rabes, et al.: Climate reconstruction for the last two](#)
618 [millennia in central Iberia: The role of East Atlantic \(EA\), North Atlantic Oscillation \(NAO\)](#)
619 [and their interplay over the Iberian Peninsula. *Quaternary Science Reviews*, 149, 135–150,](#)
620 [2016.](#)

621 Server, M.: Evaluation of an oral history text in the context of social memory and traditional
622 activity, *Milli Folklor* 77, 61–68 (In Turkish), 2008.

623 Speer, J. H.: *Fundamentals of Tree-Ring Research*, University of Arizona Press, Tucson, 2010.

624 [St. George, S.: An overview of tree-ring width records across the Northern Hemisphere, *Quat.*](#)
625 [*Sci. Rev.*, 95, 132–150, 2014.](#)

626 [St. George, S., and Ault, T. R.: The imprint of climate within northern hemisphere trees, *Quat.*](#)
627 [*Sci. Rev.*, 89, 1–4, 2014.](#)

628 Stokes, M. A. and Smiley, T. L.: *An Introduction to Tree-ring Dating*, The University of Arizona
629 Press, Tucson, 1996.

630 Till, C. and Guiot, J.: Reconstruction of precipitation in Morocco since A D 1100 based on
631 *Cedrus atlantica* tree-ring widths, *Quat. Res.*, 33, 337–351, 1990.

632 Touchan, R., Garfin, G. M., Meko, D. M., Funkhouser, G., Erkan, N., Hughes, M. K., and
633 Wallin, B. S.: Preliminary reconstructions of spring precipitation in southwestern Turkey
634 from tree-ring width, *Int. J. Clim.*, 23, 157–171, 2003.

635 Touchan, R., Xoplaki, E., Funkhouser, G., Luterbacher, J., Hughes, M. K., Erkan, N., Akkemik,
636 Ü., and Stephan, J.: Reconstruction of spring/summer precipitation for the Eastern
637 Mediterranean from tree-ring widths and its connection to large-scale atmospheric
638 circulation, *Clim. Dynam.*, 25, 75–98, 2005a.

639 Touchan, R., Funkhouser, G., Hughes, M. K., and Erkan, N.: Standardized Precipitation Index
640 reconstructed from Turkish ring widths, *Clim. Change*, 72, 339-353, 2005b.

641 Touchan, R., Akkemik, Ü., Huges, M. K., and Erkan, N.: May–June precipitation reconstruction
642 of southwestern Anatolia, Turkey during the last 900 years from tree-rings, *Quat. Res.*, 68,
643 196-202, 2007.

644 Turkes, M.: Spatial and temporal analysis of annual rainfall variations in Turkey. *Int. J. Clim.*,
645 16, 1057–1076, 1996a.

646 [Turkes, M.: Meteorological drought in Turkey: a historical perspective, 1930-1993. In: Drought](#)
647 [Network News, International Drought Information Center, University of Nebraska, 8, pp. 17-](#)
648 [21, 1996b.](#)

649 Turkes, M.: Vulnerability of Turkey to desertification with respect to precipitation and aridity
650 conditions. *Turk. J. Engineer. Environ Sci.*, 23, 363–380, 1999.

651 Turkes, M. and Sumer, U. M.: Spatial and temporal patterns of trends variability in diurnal
652 temperature ranges of Turkey. *Theor. Appl. Clim.*, 77, 195–227, 2004.

653 [Xoplaki, E., Luterbacher J., Paeth H., Dietrich, D., Grosjean, M., Wanner, H.: European spring](#)
654 [and autumn temperature variability and change of extremes over the last half millennium.](#)
655 [*Geophys. Res. Lett.*, 32, L15713, doi:10.1029/2005GL023424.](#)

656 Wahl, E. R., Anderson, D. M., Bauer, B. A., Buckner, R., Gille, E. P., Gross, W. S., Hartman,
657 M., and Shah, A.: An archive of high-resolution temperature reconstructions over the past
658 two millennia, *Geochem. Geophys. Geosyst.*, 11, Q01001, doi:10.1029/2009GC002817,
659 2010.

660 Wigley, T. M. L., Briffa, K. R., and Jones, P. D.: On the average value of correlated time series
661 with applications in dendroclimatology and hydrometeorology, *J. Clim. Appl. Met.*, 23, 201–
662 213, 1984.

663 Yamaguchi, D. K.: A simple method for cross-dating increment cores from living trees. *Can. J.*
664 *For. Res.*, 21, 414–416, 1991.

665 [Zücher, E. J.: Turkey: A modern history. Oxford Publishing Services, New York, 2004.](#)

666 Table 1. Site information for the new chronologies developed by this study in Turkey.

Site name	Site code	Species	No. trees/ cores	Aspect	Elev. (m)	Lat. (N)	Long. (E)
Çorum, Kargı, Karakise kayalıkları	KAR	<i>Pinus nigra</i>	22 / 38	SW	1522	41°11'	34°28'
Çorum, Kargı, Şahinkayası mevki	SAH	<i>P. nigra</i>	12 / 21	S	1300	41°13'	34°47'
Bilecik, Muratdere	ERC	<i>P. nigra</i>	12 / 25	SE	1240	39°53'	29°50'
Bolu, Yedigöller, Ayıkaya mevki	BOL	<i>P. sylvestris</i>	10 / 20	SW	1702	40°53'	31°40'
Eskişehir, Mihalıççık, Savaş alanı mevkii	SAV	<i>P. nigra</i>	10 / 18	S	1558	39°57'	31°12'
Kayseri, Aladağlar milli parkı, Hacer ormanı	HCR	<i>P. nigra</i>	18 / 33	S	1884	37°49'	35°17'
Kahramanmaraş, Göksun, Payanburnu mevkii	PAY	<i>P. nigra</i>	10 / 17	S	1367	37°52'	36°21'
Artvin, Borçka, Balcı işletmesi	ART	<i>Abies nordmanniana</i> <i>Picea orientalis</i>	23 / 45	N	1200– 2100	41°18'	41°54'

667

668

669 Table 2. Summary statistics for the new chronologies developed by this study in Turkey.

Site Code	Total chronology			Common interval		
	Time span	1st year (*EPS > 0.85)	Mean sensitivity	Time span	Mean correlations: among radii /between radii and mean	Variance explained by PC1 (%)
KAR	1307–2003	1620	0.22	1740–1994	0.38 / 0.63	41
SAH	1663–2003	1738	0.25	1799–2000	0.42 / 0.67	45
ERC	1721–2008	1721	0.23	1837–2008	0.45 / 0.69	48
BOL	1752–2009	1801	0.18	1839–1994	0.32 / 0.60	36
SAV	1630–2005	1700	0.17	1775–2000	0.33 / 0.60	38
HCR	1532–2010	1704	0.18	1730–2010	0.38 / 0.63	40
PAY	1537–2010	1790	0.18	1880–2010	0.28 / 0.56	32
ART	1498–2007	1624	0.12	1739–1996	0.37 / 0.60	41

670 *EPS = Expressed Population Signal [Wigley et al., 1984]

671

672 Table 3. [Principal components analysis statistics for the Turkey temperature reconstruction](#)
 673 [model.Statistics from reconstruction model principal components analysis.](#)

	Explained variance (%)	Correlation coefficients with		The chronologies represented by higher magnitudes** in the eigenvectors
		May–August PPT	March–April TMP	
PC1	46.57	0.65	0.19	KAR, KIZ, TEF, BON, USA, TUR, CAT, INC, ERC, YAU, SAV, TAN, SIU
PC2	7.86	-0.07	0.15	KAR, SAV, TIR, BOL, YAU, ESK, TEF, BON, SIU
PC3*	4.93	0.04	-0.48	HCR, PAY, BOL, YAU, SIA
PC4*	4.68	0.11	0.17	TEF, KEL, FIR, SIA, KIZ, SIU, ART
PC5*	4.42	-0.25	0.27	SAH, TIR, FIR, ART
PC6	3.73	0.15	-0.14	KIZ, FIR, SAV, KAR, TIR, PAY, ESK, TEF, BON, ART
PC7*	3.56	0.19	0.18	KIZ, BON, BOL, YAU, HCR, PAY, INC
PC8	2.87	0.26	0.01	HCR, ESK, BON, FIR, ERC, SIA
PC9*	2.45	0.16	0.17	PAY, USA, BOL, YAU, TIR, HCR, FIR, SIA, SIU
PC10*	2.21	0.14	-0.08	TUR, CAT, SAV, SIA, KEL, ERC, SIU
PC11	2.09	-0.36	-0.20	HCR, TEF, USA, INC, PAY, TUR, SAV, SIU
PC12	1.80	-0.12	0.05	TEF, CAT, YAU HCR, ESK, USA, BOL, SIA
PC13	1.63	-0.06	0.17	TEF, TUR, BOL, KAR, YAU, SIA
PC14	1.55	-0.14	0.06	TIR, USA, FIR, TUR, YAU, KAR, BON
PC15*	1.50	-0.20	-0.14	KIZ, BON, USA, ESK, INC, BOL
PC16	1.31	0.04	0.08	SAH, HCR, INC, YAU, SAV, KAR, FIR, BOL, SIU
PC17*	1.25	0.15	0.19	SAH, SIU, KAR, ESK, TUR, ERC
PC18	1.14	0.13	0.02	KAR, TEF, TUR, SAV, BON, CAT
PC19	1.09	0.16	-0.11	PAY, INC, SAV, HCR, KEL, CAT, TAN
PC20	0.95	-0.15	-0.01	TIR, SAH, CAT
PC21*	0.89	0.06	-0.28	TUR, INC, TIR, SAV
PC22	0.85	0.44	0.10	KIZ, SAH, BON, YAU, SIU
PC23	0.67	-0.22	-0.02	TAN, KEL, TUR, CAT

674 “*” indicates the PCs, which used in the reconstruction as predictors

675 “**” which exceed ± 0.2 value.

676

677

678

679

680

681 Table 4. Calibration and verification statistics of bootstrap method (1000 iterations

682 applied) showing the mean values based on the 95% confidence interval (CI).

683

		Mean (95% CI)
Calibration	RMSE	0.65 (0.52; 0.77)
	R^2	0.73 (0.60; 0.83)
Verification	RE	0.54 (0.15; 0.74)
	CE	0.51 (0.04; 0.72)
	RMSEP	0.88 (0.67; 1.09)

684 *RMSE* root mean squared error; R^2 coefficient of determination; *RE* reduction of error; *CE*

685 coefficient of efficiency; *RMSEP* root mean squared error prediction

686

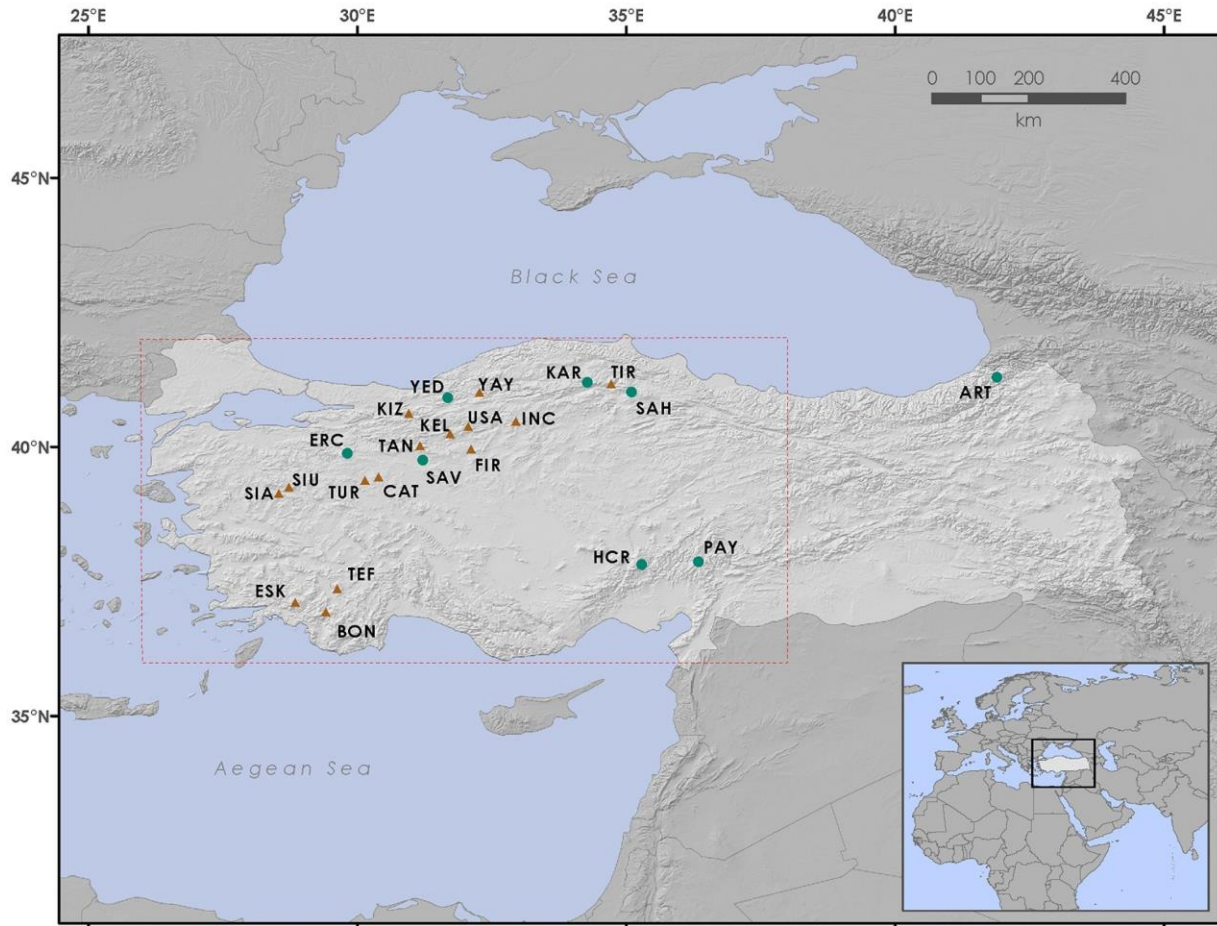
687 Table 5. [Calibration and cross-validation statistics for the Turkey temperature reconstruction](#)
688 [model. Results of the statistical calibrations and cross-validations](#)

Calibration Period	Verification Period	Adj. R^2	F	RE	CE
1930–1966	1967–2002	0.55	5.91	0.64	0.58
$p \leq 0.0001$					
1967–2002	1930–1966	0.71	10.45	0.63	0.46
$p \leq 0.0001$					

689

690

691

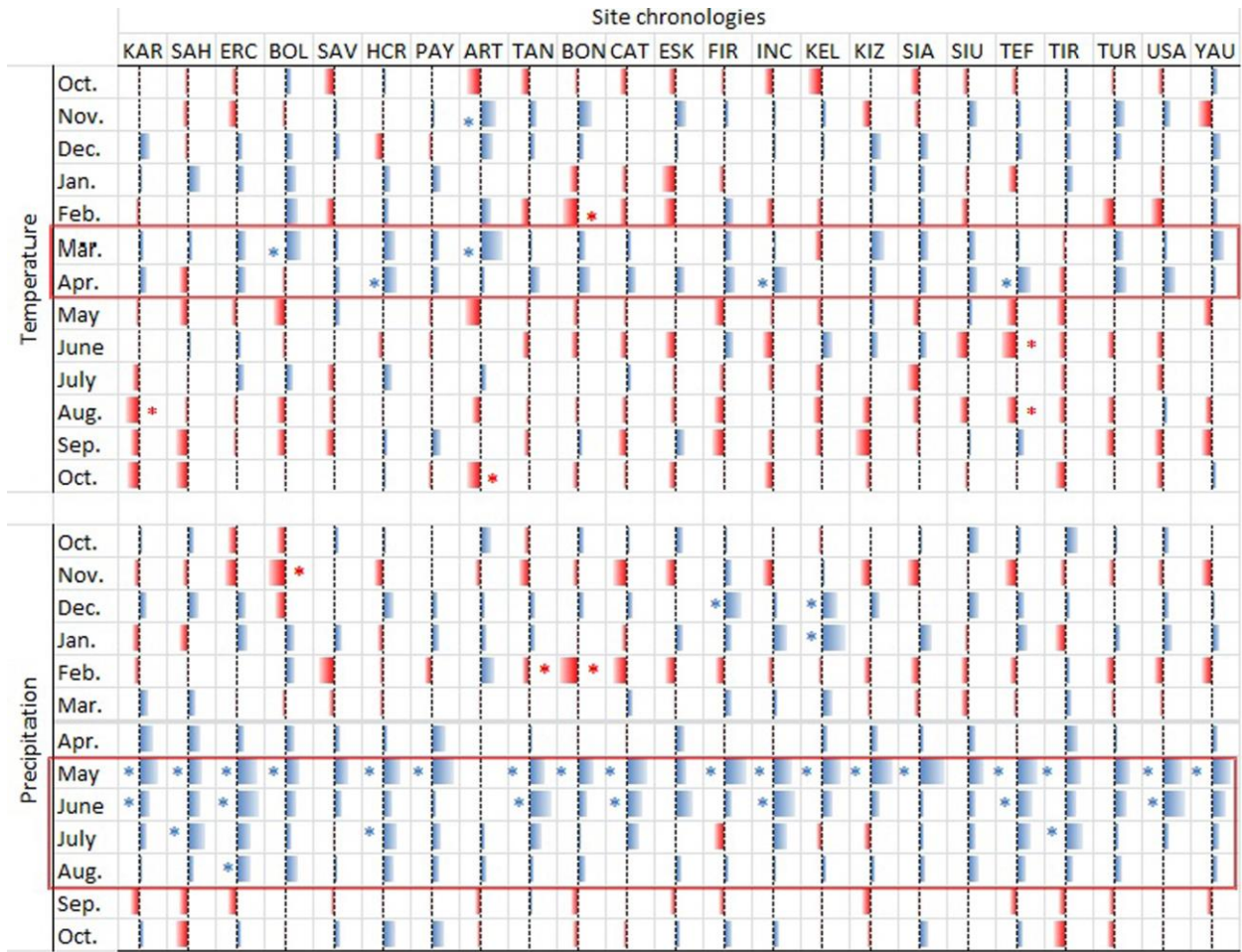


692 **Figure 1.** Tree-ring chronology sites in Turkey used to reconstruct temperature. Circles
693 represent the new sampling efforts from this study and the triangles represent previously-
694 published chronologies (YAY, SIA, SIU: Mutlu et al. 2011; TIR: Akkemik et al. 2008; TAN:
695 Köse et al. unpublished data; KIZ, ESK, TEF, BON, KEL, USA, FIR, TUR: Köse et al. 2011;
696 CAT, INC: Köse et al. 2005). The box (dashed line) represents the area for which the
697 temperature reconstruction was performed.
698

699

700

701



702

703

Figure 2. Summary of response function results of 23 chronologies. Red color represents

704

negative effects of climate variability on tree ring width; blue color represents positive effects of

705

climate variability on tree ring width. “*” indicates statistically significant response function

706

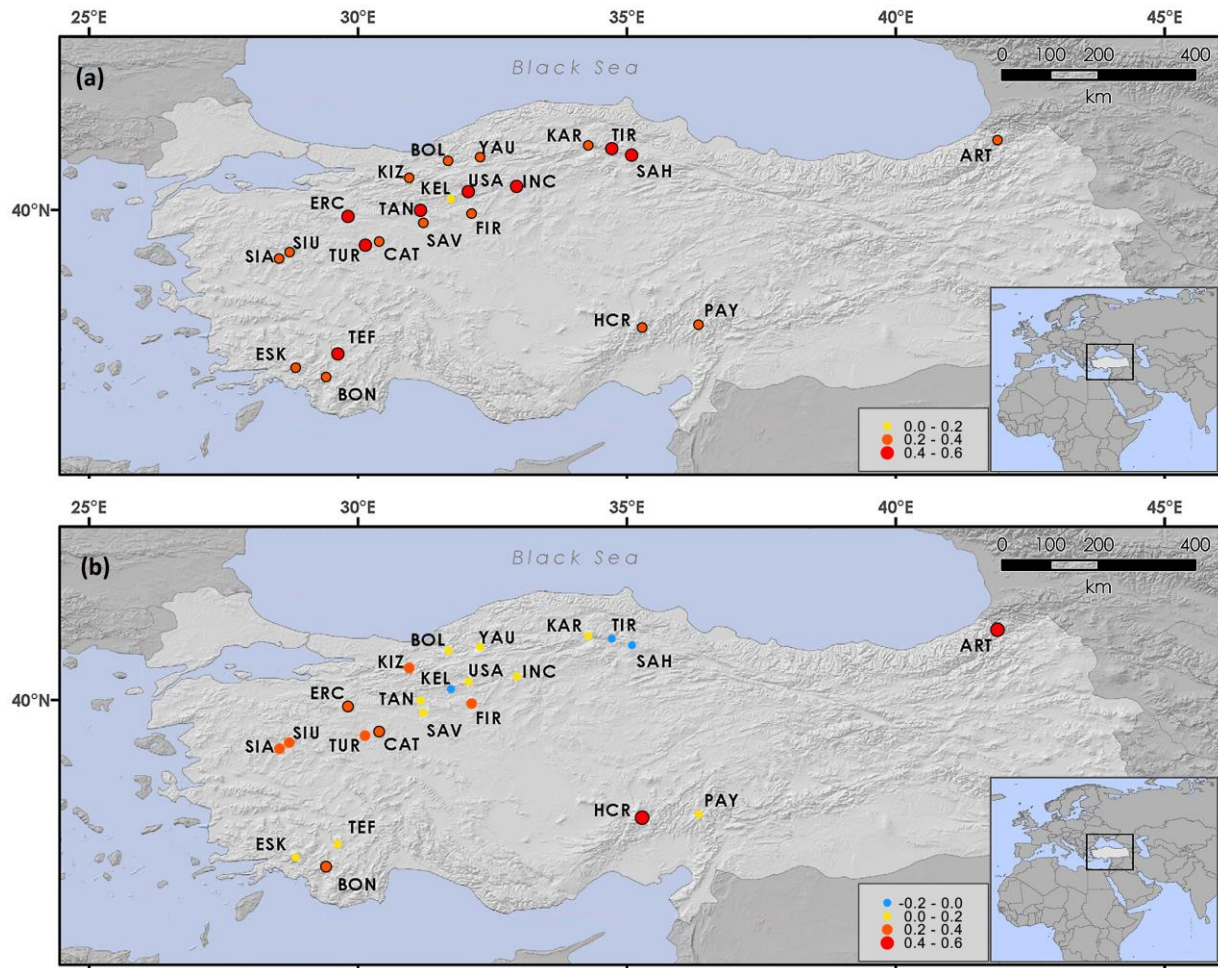
confidents ($p \leq 0.05$). Each response function includes 13 weights for average monthly

707

temperatures and 13 monthly precipitations from October of the prior year to October of current

708

year.



709

710 **Figure 3.** Maps showing Pearson's correlation coefficients between the sites chronologies and

711 (a) May - August total precipitation and (b) March-April mean temperature for the period 1930-

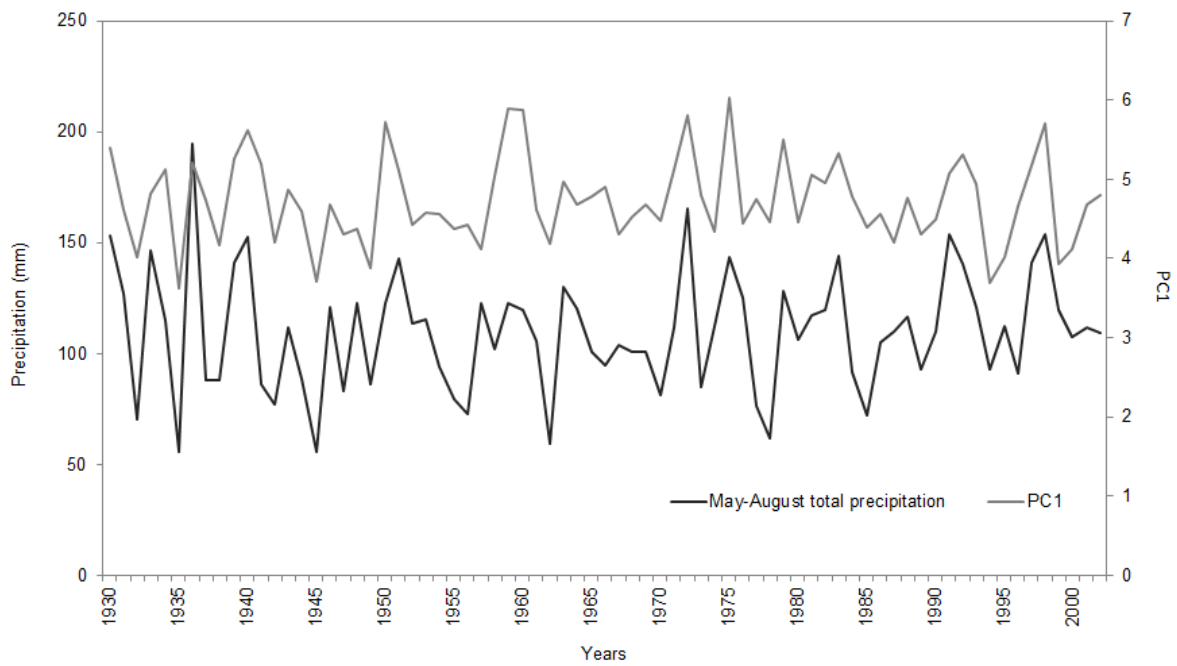
712 2012. For each site, the closest gridded (0.5° x 0.5°) climate data obtained from CRU dataset

713 were used. Graduated circle size and color correspond to correlation coefficient versus the

714 climate variable. Black lines surrounding circles represent significant correlation coefficients

715 ($p < 0.05$).

716



717

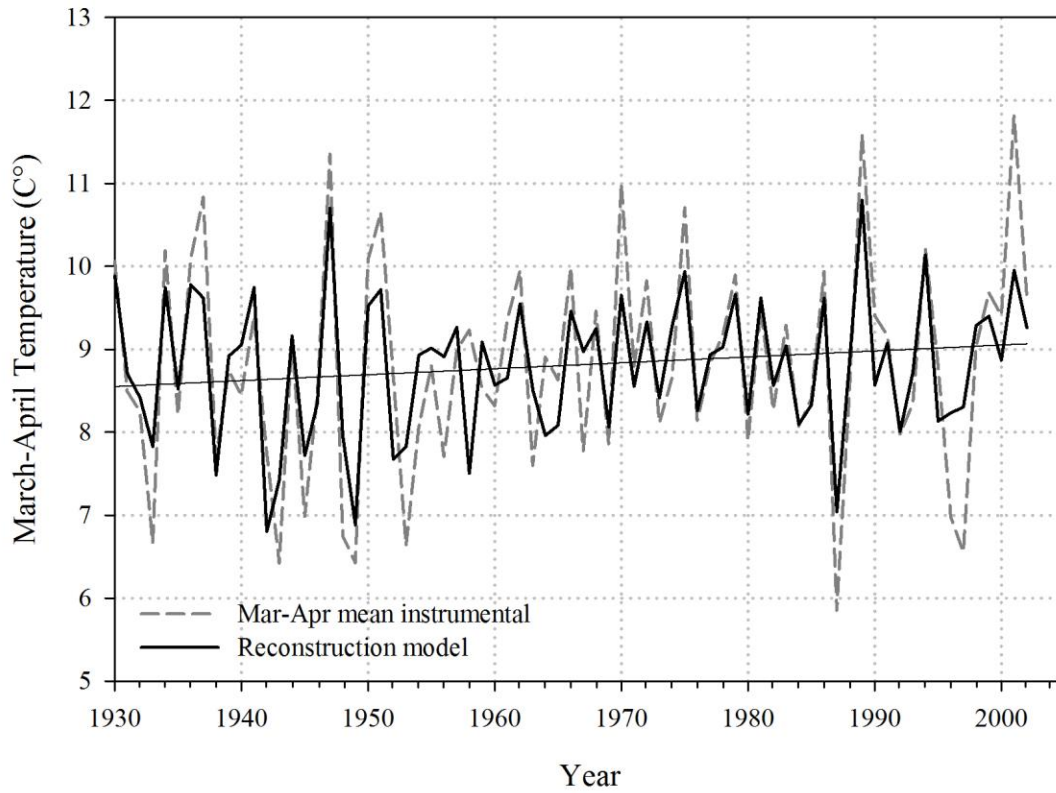
718 **Figure 34.** The comparison of May-August total precipitation (mm) and the first principal
 719 component of 23 tree-ring chronologies.

720

721

722

723



724

725 **Figure 45.** Actual (instrumental) and reconstructed March–April temperature (°C). Dashed lines
 726 (dark grey) represent actual values and solid lines (black) represent reconstructed values shown
 727 with trend line (linear black line). Note: y-axes labels range 5–13 °C.

728

729

730

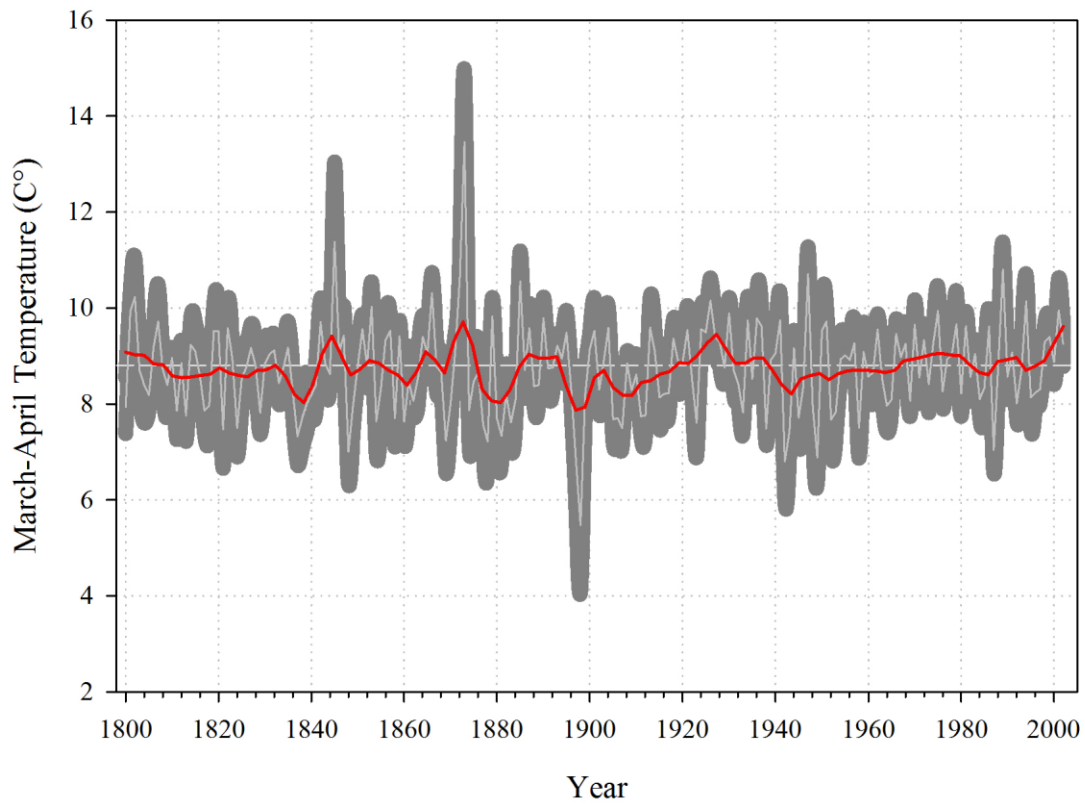
731

732

733

734

735



736

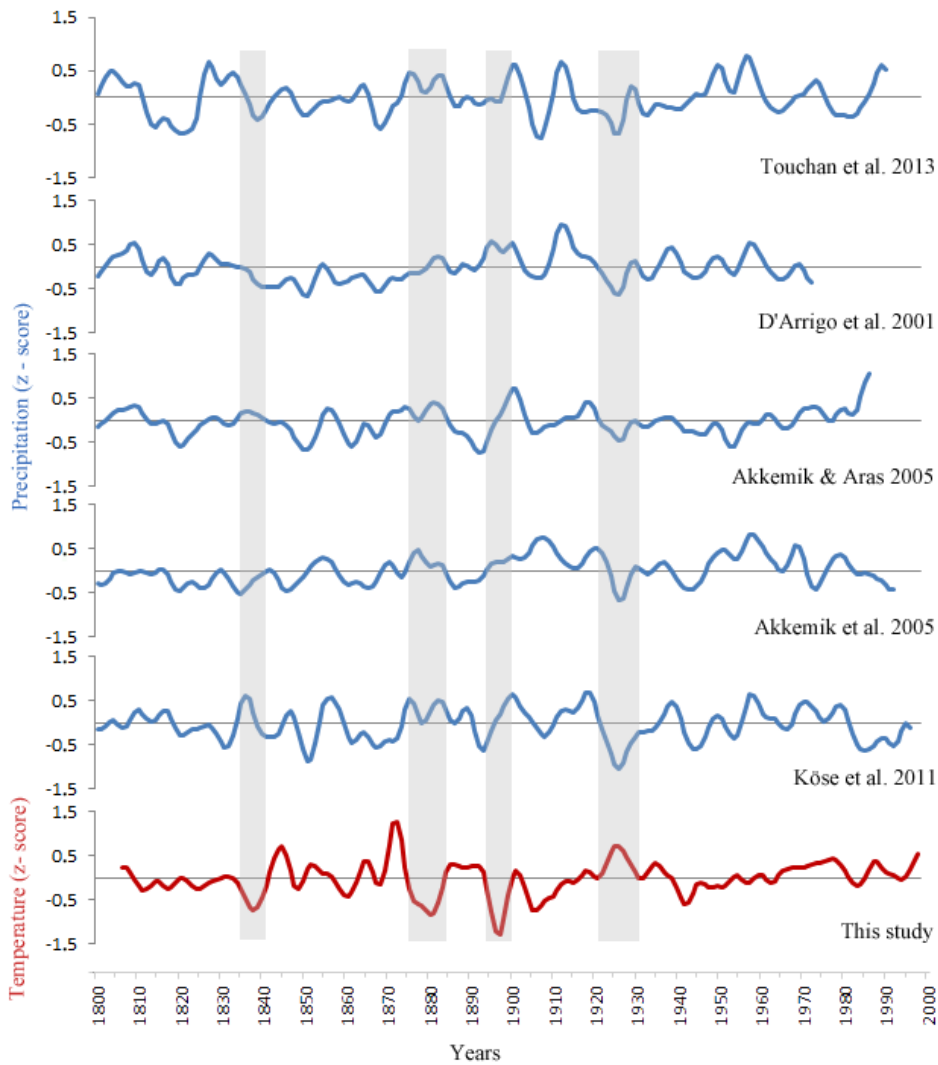
737 **Figure 56.** March–April temperature reconstruction for Turkey for the period 1800–2002
 738 CE. The central horizontal line (dashed white) shows the reconstructed long-term mean;
 739 dark grey background denotes Monte Carlo ($n = 1000$) bootstrapped 95% confidence
 740 limits; and the solid black line shows 13-year low-pass filter values. Note: y-axis labels
 741 range 2–16 °C.

742

743

744

745



746

747

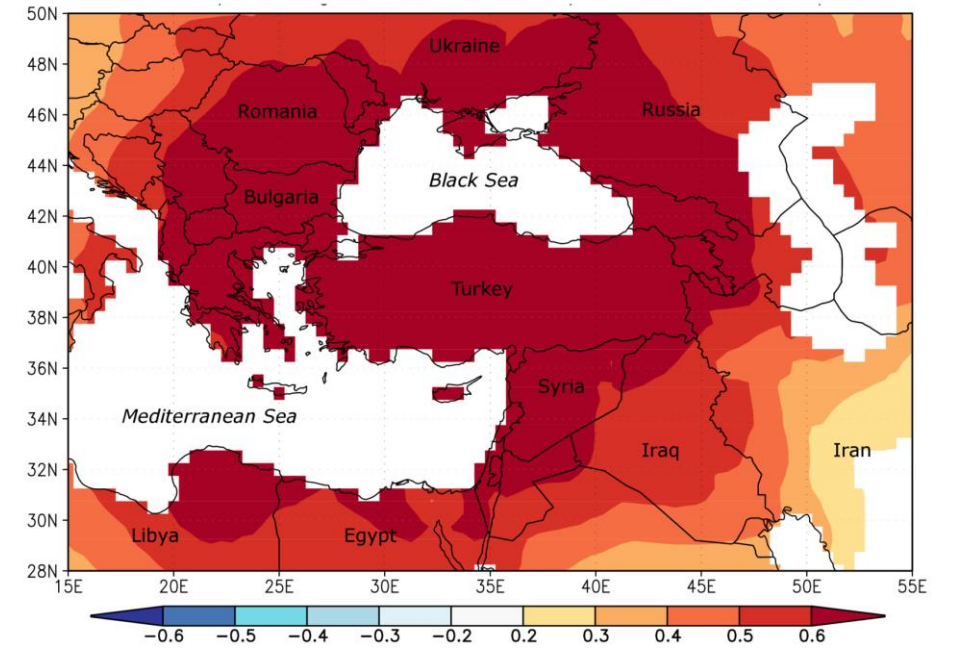
Figure 7. Low-frequency variability of previous tree-ring based precipitation

748

reconstructions from Turkey and spring temperature reconstruction. Each line shows 13-

749

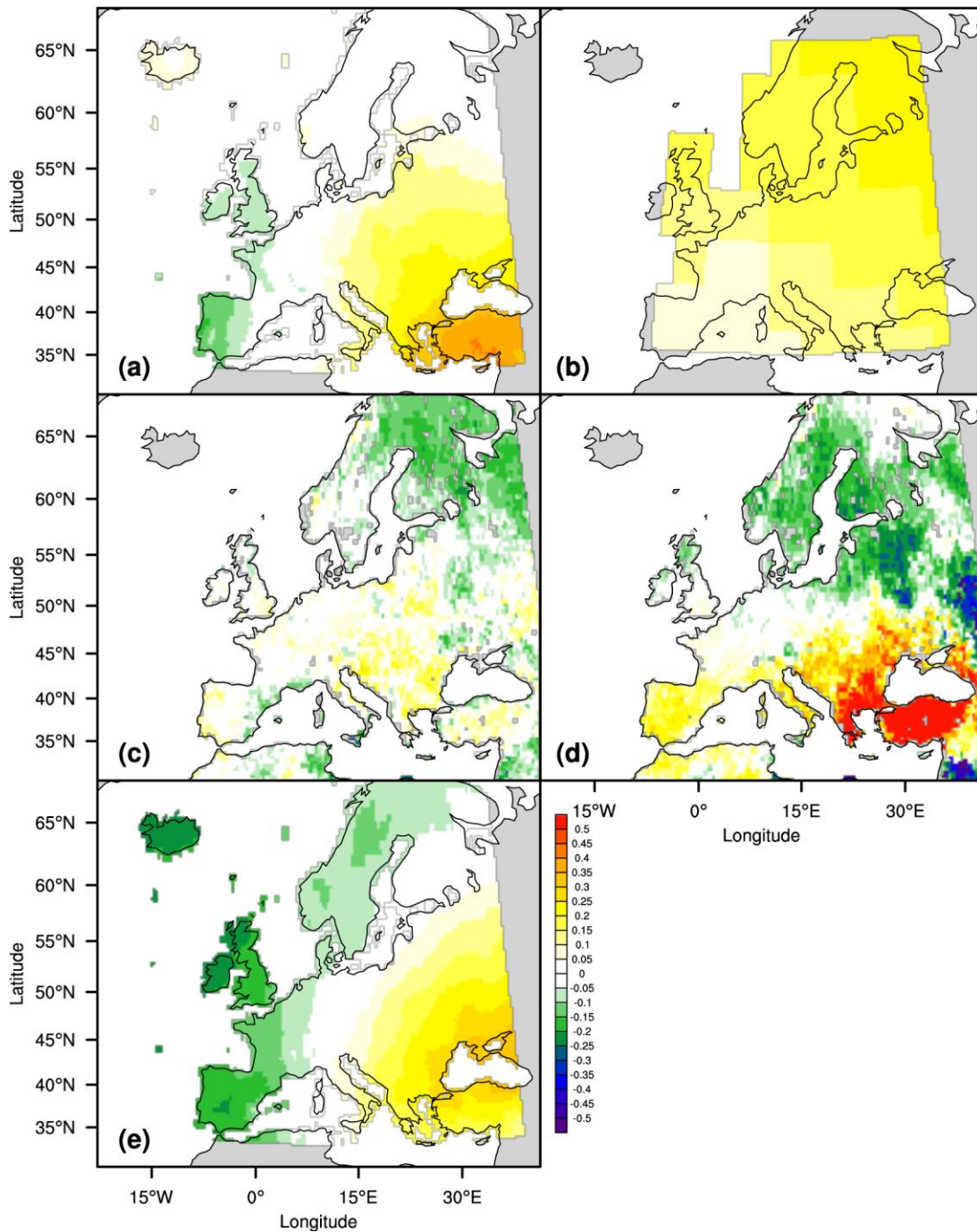
year low-pass filter values. z-scores were used for comparison.



750

751 **Figure 8.** Spatial correlation map for the March–April temperature reconstruction. Spatial
 752 field correlation map showing statistical relationship between the temperature
 753 reconstruction and the gridded temperature field at 0.5° intervals (CRU TS3.23; Jones and
 754 Harris 2008) during the period 1930–2002 over the Mediterranean region.

755



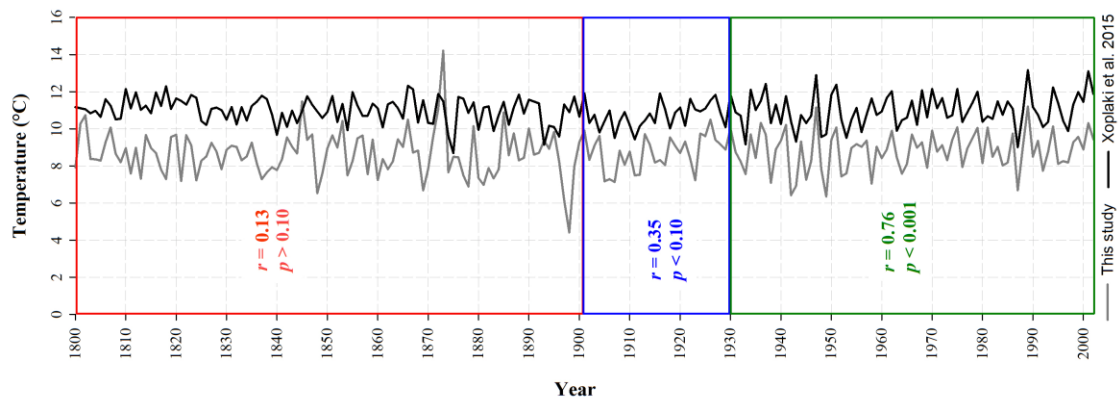
756

757

758

Figure 9. Spatial correlation maps for the March–April temperature reconstruction and precipitation signal (PC1) obtained from tree-ring data set during the period 1800–2002

759 over Europe. Maps demonstrate spatial field correlations between our temperature
760 reconstruction and (a) gridded spring temperature reconstruction for Europe (Xoplaki et al.
761 2005), (b) gridded summer temperature reconstruction for Europe (Luterbacher et al. 2016), (c)
762 Old World Drought Atlas (OWDA; Cook et al. 2015). Panels (d) and (e) show spatial
763 correlations between PC1 and OWDA (Cook et al. 2015) and gridded European summer
764 precipitation reconstruction (Pauling et al., 2006), respectively.
765



766
767 **Figure 10.** Comparison of March-April temperature reconstruction with the mean of
768 corresponding grid points from European spring temperature reconstruction over the study area
769 (36–42° N, 26–38° E).
770
771